



Scalar conservation laws with moving constraints arising in traffic flow modeling: an existence result

Maria Laura Delle Monache, Paola Goatin

► To cite this version:

Maria Laura Delle Monache, Paola Goatin. Scalar conservation laws with moving constraints arising in traffic flow modeling: an existence result. *Journal of Differential Equations*, 2014, 257, pp.4015-4029. hal-00976855

HAL Id: hal-00976855

<https://hal.inria.fr/hal-00976855>

Submitted on 10 Apr 2014

HAL is a multi-disciplinary open access archive for the deposit and dissemination of scientific research documents, whether they are published or not. The documents may come from teaching and research institutions in France or abroad, or from public or private research centers.

L'archive ouverte pluridisciplinaire **HAL**, est destinée au dépôt et à la diffusion de documents scientifiques de niveau recherche, publiés ou non, émanant des établissements d'enseignement et de recherche français ou étrangers, des laboratoires publics ou privés.

Scalar conservation laws with moving constraints arising in traffic flow modeling: an existence result

M. L. Delle Monache^{a,*}, P. Goatin^a

^a*INRIA Sophia Antipolis - Méditerranée, EPI OPALE, Sophia Antipolis, (FRANCE)*

Abstract

We consider a strongly coupled PDE-ODE system that describes the influence of a slow and large vehicle on road traffic. The model consists of a scalar conservation law accounting for the main traffic evolution, while the trajectory of the slower vehicle is given by an ODE depending on the downstream traffic density. The moving constraint is expressed by an inequality on the flux, which models the bottleneck created in the road by the presence of the slower vehicle. We prove the existence of solutions to the Cauchy problem for initial data of bounded variation.

Keywords: Scalar conservation laws with constraints, Traffic flow modeling, PDE-ODE coupling, Wave-front tracking approximations.
2010 MSC: 35L65, 90B20

1. Introduction

A slow moving large vehicle, like a bus or a truck, reduces the road capacity and thus generates a moving bottleneck for the surrounding traffic flow. This situation can be modeled by a PDE-ODE strongly coupled system consisting of a scalar conservation law with moving flux constraint accounting for traffic evolution and an ODE describing the slower vehicle motion, i.e.

$$\begin{cases} \partial_t \rho + \partial_x f(\rho) = 0, & (t, x) \in \mathbb{R}^+ \times \mathbb{R}, \\ \rho(0, x) = \rho_o(x), & x \in \mathbb{R}, \\ f(\rho(t, y(t))) - \dot{y}(t)\rho(t, y(t)) \leq \frac{\alpha R}{4V}(V - \dot{y}(t))^2 & t \in \mathbb{R}^+, \\ \dot{y}(t) = \omega(\rho(t, y(t)+)), & t \in \mathbb{R}^+, \\ y(0) = y_o. \end{cases} \quad (1)$$

Above, $\rho = \rho(t, x) \in [0, R]$ is the mean traffic density, R the maximal density allowed on the road and the flux function $f : [0, R] \rightarrow \mathbb{R}^+$ is a strictly concave

*Corresponding author

Email addresses: maria-laura.delle_monache@inria.fr (M. L. Delle Monache),
paola.goatin@inria.fr (P. Goatin)

function such that $f(0) = f(R) = 0$, see Figure 1a. It is given by the following flux-density relation

$$f(\rho) = \rho v(\rho),$$

where v is a smooth decreasing function denoting the mean traffic speed. In this paper, we will take $v(\rho) = V(1 - \rho/R)$, V being the maximal velocity allowed on the road.

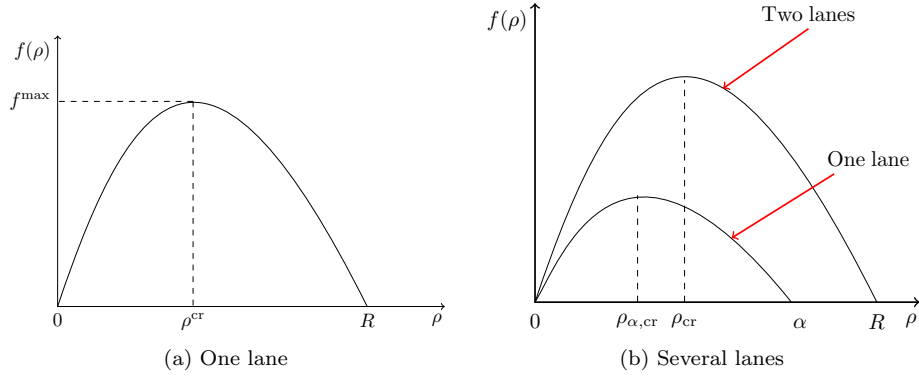


Figure 1: A typical example of flux function for traffic flow (left). Every road has a specific fundamental diagram. For roads with different number of lanes we can consider that the fundamental diagrams are in a ratio corresponding to their maximal capacities (right).

The time-dependent variable y denotes the bus position. When the traffic conditions allow it, the bus moves at its own maximal speed denoted by $V_b < V$. When the surrounding traffic is too dense, the bus adapts its velocity accordingly, therefore it is not possible for the bus to overtake the cars, see Figure 2. From a mathematical point of view, the velocity of the bus can be described by a traffic density dependent speed of the form:

$$\omega(\rho) = \begin{cases} V_b & \text{if } \rho \leq \rho^* \doteq R(1 - V_b/V), \\ v(\rho) & \text{otherwise.} \end{cases} \quad (2)$$

Model (1) was introduced in [16] to describe the effects of urban transport systems in a road network. Other macroscopic models for moving bottlenecks in road traffic were recently proposed in [2, 18]. Compared to those approaches, the model described here offers a more realistic definition of the slower vehicle speed, and a description of its impact on traffic conditions which is simpler to handle both analytically and numerically.

From the analytical point of view, the model can be viewed as a generalization to moving constraints of the problem consisting in a scalar conservation law with a (fixed in space) constraint on the flux, introduced and studied in

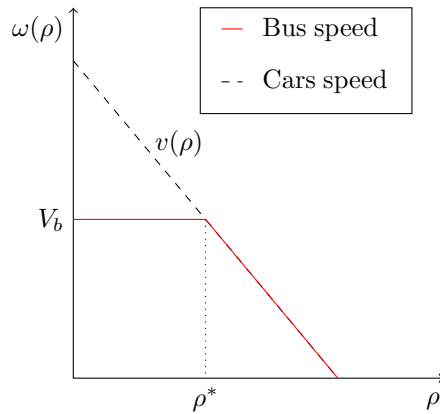


Figure 2: Bus and cars speed.

[1, 9, 8], see also [15] for an extension to systems. In the present case, the constraint location moves due to the surrounding traffic conditions, which in turn are modified by the presence of the slower vehicle, thus resulting in a strong non-trivial coupling between the conservation equation and the trajectory of the vehicle.

The study of coupled PDE-ODE systems is not new in the conservation laws framework, we refer the reader to [3, 7, 10, 18]. Nevertheless, the problem posed here is slightly different. On one side, we deal with a strong coupling with the PDE and the ODE affecting each other, unlike [7, 10], where the PDE solution does not depend on the ODE. On the other side, even if the ODE has discontinuous right-hand side, the particular definition of the model allows us to consider classical Carathéodory solutions, as in [3, 2, 4, 7], instead of the weaker Filippov's generalized solutions needed in [10, 18].

Some numerical methods related to (1) have been developed in [11, 12, 13]. In particular, in [11, 12] the moving constraints are replaced by a sequence of fixed ones and the discontinuity is applied at the upstream cell interface with respect to the bottleneck position. The main disadvantage of this approach is that the approximate flows, densities and speeds at a point do not converge to the exact ones. Hence, to provide the necessary estimates one needs to average their values over multiple cells. In [13] we introduce a Lagrangian algorithm that follows the bus position with a non-uniform moving mesh.

In this article, we provide an existence result for the Cauchy problem with data of bounded variation, as stated by Theorem 1 in Section 4. The proof relies on wave-front tracking approximations. The stability of solutions with respect to the initial data is still an open problem.

The article is organized as follows. Section 2 gives a description of the model from an analytic point of view, Section 3 is dedicated to the solution of the Riemann problem and Section 4 contains the proof of the existence result for the Cauchy problem.

2. Model derivation

To describe the interaction between the bus and the traffic we consider the bus as a mobile obstacle, i.e., as a moving restriction of the road. The situation is the following: upstream and downstream with respect to the bus, the cars behave normally while besides the bus the road capacity is reduced, generating a bottleneck, see Figure 3.

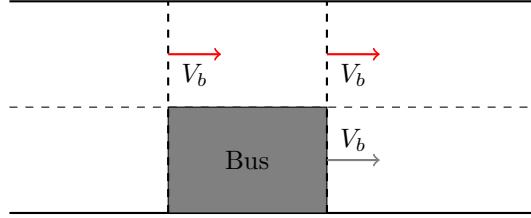


Figure 3: Moving bottleneck.

This pointwise discontinuity moves at the bus speed. To better capture the influence of the bus, we choose to study the problem in the bus reference frame, which means setting $X = x - y(t)$. In this coordinate system, the velocity of the bus is equal to zero and the conservation law becomes:

$$\partial_t \rho + \partial_X (f(\rho) - \dot{y}\rho) = 0. \quad (3)$$

The corresponding constraint on the flux can be written as

$$f(\rho(t, y(t))) - \dot{y}(t)\rho(t, y(t)) \leq \frac{\alpha R}{4V} (V - \dot{y}(t))^2, \quad (4)$$

with the constant coefficient $\alpha \in]0, 1[$ giving the reduction rate of the road capacity due to the presence of the bus. Indeed, let $f_\alpha : [0, \alpha R] \rightarrow \mathbb{R}^+$ be the rescaled flux function describing the reduced flow at $x = y(t)$, i.e.

$$f_\alpha(\rho) = V\rho \left(1 - \frac{\rho}{\alpha R}\right),$$

and $\rho_\alpha \in]0, \alpha R/2[$ such that $f'_\alpha(\rho_\alpha) = \dot{y}$, i.e.

$$\rho_\alpha = \frac{\alpha R}{2} \left(1 - \frac{\dot{y}}{V}\right),$$

see Figure 4. Therefore, the right-hand side of (4) is given by

$$f_\alpha(\rho_\alpha) - \dot{y}\rho_\alpha = \frac{\alpha R}{4V} (V - \dot{y}(t))^2.$$

Note that inequality (4) is always satisfied if $\dot{y}(t) = v(\rho)$, since the left hand side is 0. Moreover, it is well defined even if ρ has a jump at $y(t)$ because of the Rankine-Hugoniot conditions.

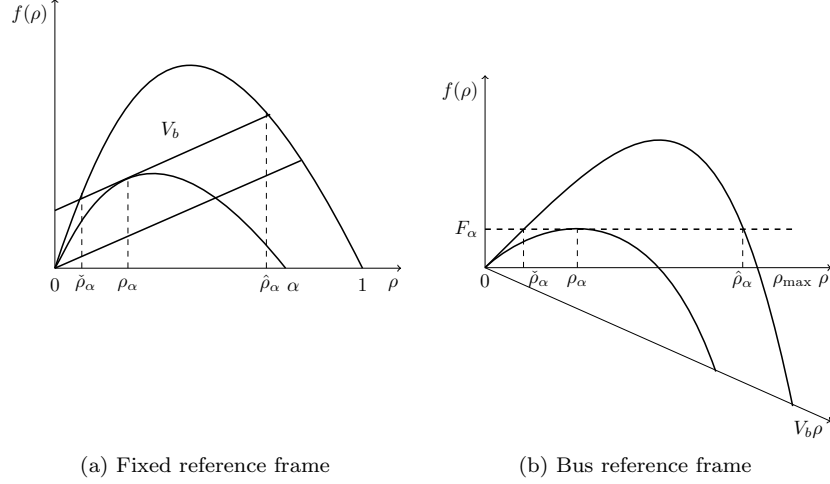


Figure 4: Flux functions for $\dot{y} = V_b$. The big fundamental diagram describes the whole road and, the smaller one, the constrained flux at the bus location.

For our analytical purposes, it is not restrictive to assume that $R = V = 1$, so that the model becomes

$$\begin{cases} \partial_t \rho + \partial_x(\rho(1 - \rho)) = 0, & (t, x) \in \mathbb{R}^+ \times \mathbb{R}, \\ \rho(0, x) = \rho_o(x), & x \in \mathbb{R}, \\ f(\rho(t, y(t))) - \dot{y}(t)\rho(t, y(t)) \leq \frac{\alpha}{4}(1 - \dot{y}(t))^2 := F_\alpha & t \in \mathbb{R}^+, \\ \dot{y}(t) = \omega(\rho(t, y(t)+)), & t \in \mathbb{R}^+, \\ y(0) = y_o. \end{cases} \quad (5)$$

We will refer to this system in the following sections.

3. The Riemann problem with moving density constraint

We devote this section to the study of the Riemann problem. Consider (5) with Riemann type initial data

$$\rho_o(x) = \begin{cases} \rho_L & \text{if } x < 0, \\ \rho_R & \text{if } x > 0, \end{cases} \quad \text{and } y_o = 0. \quad (6)$$

We aim at defining a Riemann solver for the conservation law with moving flux constraint. Therefore we consider the following Riemann problem

$$\begin{cases} \partial_t \rho + \partial_x f(\rho) = 0, \\ \rho(0, x) = \begin{cases} \rho_L & \text{if } x < 0, \\ \rho_R & \text{if } x > 0, \end{cases} \end{cases} \quad (7)$$

under the constraint

$$f(\rho(t, y(t))) - \dot{y}(t)\rho(t, y(t)) \leq \frac{\alpha}{4}(1 - \dot{y}(t))^2,$$

where the bus velocity $\dot{y}(t)$ is assumed to be constant by self-similarity.

The definition of the Riemann solver for (5), (6) follows [16, §V]. Denote by \mathcal{R} the standard (i.e., without the constraint (4)) Riemann solver for (7), i.e., the (right continuous) map $(t, x) \mapsto \mathcal{R}(\rho_L, \rho_R)(x/t)$ given by the standard weak entropy solution to (7). Moreover, let $\check{\rho}_\alpha$ and $\hat{\rho}_\alpha$, with $\check{\rho}_\alpha \leq \hat{\rho}_\alpha$, be the intersection points of the flux function $f(\rho)$ with the line $f_\alpha(\rho_\alpha) + V_b(\rho - \rho_\alpha)$ (see Figure 4).

Definition 3.1. *The constrained Riemann solver $\mathcal{R}^\alpha : [0, 1]^2 \rightarrow \mathbf{L}_{\text{loc}}^1(\mathbb{R}; [0, 1])$ for (5), (6) is defined as follows.*

1. If $f(\mathcal{R}(\rho_L, \rho_R)(V_b)) > F_\alpha + V_b \mathcal{R}(\rho_L, \rho_R)(V_b)$, then

$$\mathcal{R}^\alpha(\rho_L, \rho_R)(x/t) = \begin{cases} \mathcal{R}(\rho_L, \hat{\rho}_\alpha)(x/t) & \text{if } x < V_b t, \\ \mathcal{R}(\check{\rho}_\alpha, \rho_R)(x/t) & \text{if } x \geq V_b t, \end{cases} \quad \text{and } y(t) = V_b t.$$

2. If $V_b \mathcal{R}(\rho_L, \rho_R)(V_b) \leq f(\mathcal{R}(\rho_L, \rho_R)(V_b)) \leq F_\alpha + V_b \mathcal{R}(\rho_L, \rho_R)(V_b)$, then

$$\mathcal{R}^\alpha(\rho_L, \rho_R) = \mathcal{R}(\rho_L, \rho_R) \quad \text{and } y(t) = V_b t.$$

3. If $f(\mathcal{R}(\rho_L, \rho_R)(V_b)) < V_b \mathcal{R}(\rho_L, \rho_R)(V_b)$, then

$$\mathcal{R}^\alpha(\rho_L, \rho_R) = \mathcal{R}(\rho_L, \rho_R) \quad \text{and } y(t) = v(\rho_R)t.$$

Note that, when the constraint is enforced (point 1. in the above definition), a non-classical shock arises, which satisfies the Rankine-Hugoniot condition but violates the Lax entropy condition.

Remark 1. The above definition is well-posed even if the classical solution $\mathcal{R}(\rho_L, \rho_R)(x/t)$ displays a shock at $x = V_b t$. In fact, due to Rankine-Hugoniot equation, we have

$$f(\rho_L) = f(\rho_R) + V_b(\rho_L - \rho_R)$$

and hence

$$f(\rho_L) > f_\alpha(\rho_\alpha) + V_b(\rho_L - \rho_\alpha) \iff f(\rho_R) > f_\alpha(\rho_\alpha) + V_b(\rho_R - \rho_\alpha).$$

4. The Cauchy problem: existence of solutions

The aim of this section is to study existence of solutions of problems (1) and (5). A bus travels along a road whose traffic evolution is modeled by

$$\partial_t \rho + \partial_x(\rho(1 - \rho)) = 0, \tag{8}$$

$$\rho(0, x) = \rho_o(x), \tag{9}$$

$$f(\rho(t, y(t))) - \dot{y}(t)\rho(t, y(t)) \leq F_\alpha. \tag{10}$$

The bus influences the traffic along the road but it is also influenced by the downstream traffic conditions. The bus trajectory $y = y(t)$ then solves

$$\begin{aligned} \dot{y}(t) &= \omega(\rho(t, y(t)+)), \\ y(0) &= y_o. \end{aligned} \quad (11)$$

Solutions to (11) are intended in Carathéodory sense, i.e., as absolutely continuous functions which satisfy (11) for a.e. $t \geq 0$. Observe that the function $F(t, x) = \omega(\rho(t, x))$ is discontinuous w.r.t. x and it does not satisfy general conditions which imply well-posedness of the Cauchy problem (11), see [14, §1] for the Carathéodory conditions, and [4, 7] for ODEs which are discontinuous w.r.t. x . In particular, the bus velocity function (2) does not fulfill the assumptions in [7, (A1)-(A2)] and [10, Eq. (2.1)]. In our setting, due to the strong PDE-ODE coupling, we will prove existence and continuous dependence of both solutions to (8) and (11) at the same time.

Definition 4.1. A couple $(\rho, y) \in \mathcal{C}^0(\mathbb{R}^+; \mathbf{L}^1 \cap BV(\mathbb{R}; [0, 1])) \times \mathbf{W}^{1,1}(\mathbb{R}^+; \mathbb{R})$ is a solution to (5) if

1. ρ is a weak solution of (8), (9), i.e. for all $\varphi \in \mathcal{C}_c^1(\mathbb{R}^2; \mathbb{R})$

$$\int_{\mathbb{R}^+} \int_{\mathbb{R}} (\rho \partial_t \varphi + f(\rho) \partial_x \varphi) dx dt + \int_{\mathbb{R}} \rho_o(x) \varphi(0, x) dx = 0 ; \quad (12a)$$

moreover, ρ satisfies Kružhkov entropy conditions [17] on $(\mathbb{R}^+ \times \mathbb{R}) \setminus \{(t, y(t)) : t \in \mathbb{R}^+\}$, i.e. for every $k \in [0, 1]$ and for all $\varphi \in \mathcal{C}_c^1(\mathbb{R}^2; \mathbb{R}^+)$ and $\varphi(t, y(t)) = 0$, $t > 0$,

$$\begin{aligned} \int_{\mathbb{R}^+} \int_{\mathbb{R}} (|\rho - k| \partial_t \varphi + \text{sgn}(\rho - k) (f(\rho) - f(k)) \partial_x \varphi) dx dt \\ + \int_{\mathbb{R}} |\rho_o - k| \varphi(0, x) dx \geq 0 ; \end{aligned} \quad (12b)$$

2. y is a Carathéodory solution of (11), i.e. for a.e. $t \in \mathbb{R}^+$

$$y(t) = y_o + \int_0^t \omega(\rho(s, y(s)+)) ds ; \quad (12c)$$

3. the constraint (10) is satisfied, in the sense that for a.e. $t \in \mathbb{R}^+$

$$\lim_{x \rightarrow y(t) \pm} (f(\rho) - \omega(\rho) \rho)(t, x) \leq F_\alpha. \quad (12d)$$

Remark that the above traces exist because $\rho(t, \cdot) \in BV(\mathbb{R}; [0, 1])$ for all $t \in \mathbb{R}^+$.

Remark 2. Our choice of Carathéodory solutions for (11) is justified by the particular bus velocity defined by (2). With this choice it is not possible for the bus to end up trapped in a queue unless its speed is equal to V_b , in which case $\omega(\rho(t, y(t)+)) = \omega(\rho(t, y(t)-)) = V_b$. Therefore Carathéodory solutions are always well defined.

We are now ready to state the main result of the paper.

Theorem 1. *Let $\rho_o \in BV(\mathbb{R}; [0, 1])$, then the Cauchy problem (5) admits a solution in the sense of Definition 4.1.*

The rest of the section is devoted to the proof of Theorem 1. In particular, we will construct a sequence of approximate solutions via the wave-front tracking method, and prove its convergence. Finally we will check that the limit functions satisfy conditions (12a)-(12d) of Definition 4.1.

4.1. Wave-front tracking

To construct piecewise constant approximate solutions, we adapt the standard wave-front tracking method, see for example [5, §6]. Fix a positive $n \in \mathbb{N}$, $n > 0$ and introduce in $[0, 1]$ the mesh $\mathcal{M}_n = \{\rho_i^n\}_{i=0}^{2^n}$ defined by

$$\mathcal{M}_n = (2^{-n}\mathbb{N} \cap [0, 1]).$$

In order to include the critical points $\check{\rho}_\alpha, \hat{\rho}_\alpha$, we modify the above mesh as follows:

- if $\min_i |\check{\rho}_\alpha - \rho_i^n| = 2^{-n-1}$, then we simply add the new point to the mesh:

$$\widetilde{\mathcal{M}}_n = \mathcal{M}_n \cup \{\check{\rho}_\alpha\};$$

- if $|\check{\rho}_\alpha - \rho_l^n| = \min_i |\check{\rho}_\alpha - \rho_i^n| < 2^{-n-1}$, then we replace ρ_l^n by $\check{\rho}_\alpha$:

$$\widetilde{\mathcal{M}}_n = \mathcal{M}_n \cup \{\check{\rho}_\alpha\} \setminus \{\rho_l^n\};$$

- we perform the same operations for $\hat{\rho}_\alpha$.

In this way the distance between two points of the mesh $\widetilde{\mathcal{M}}_n = \{\tilde{\rho}_i^n\}$ satisfies the lower bound $|\tilde{\rho}_i^n - \tilde{\rho}_j^n| \geq 2^{-n-1}$.

Let f_n be the piecewise linear function which coincides with f on \mathcal{M}_n , and let ρ_o^n be a piecewise constant function defined by

$$\rho_o^n = \sum_{j \in \mathbb{Z}} \rho_{o,j}^n \chi_{[x_{j-1}, x_j]} \quad \text{with } \rho_{o,j}^n \in \widetilde{\mathcal{M}}_n,$$

which approximates ρ_o in the sense of the strong \mathbf{L}^1 topology, that is

$$\lim_{n \rightarrow \infty} \|\rho_o^n - \rho_o\|_{\mathbf{L}^1(\mathbb{R})} = 0,$$

and such that $\text{TV}(\rho_o^n) \leq \text{TV}(\rho_o)$. Above, we have set $x_0 = y_o$.

For small times $t > 0$, a piecewise approximate solution (ρ^n, y_n) to (5) is constructed piecing together the solutions to the Riemann problems

$$\begin{cases} \partial_t \rho + \partial_x (f^n(\rho)) = 0, \\ \rho(0, x) = \begin{cases} \rho_{o,0} & \text{if } x < y_o, \\ \rho_{o,1} & \text{if } x > y_o, \end{cases} \\ f(\rho(t, 0)) - \dot{y}_n(t) \rho(t, 0) \leq \frac{\alpha}{4} (1 - \dot{y}_n)^2, \end{cases} \quad \begin{cases} \partial_t \rho + \partial_x (f^n(\rho)) = 0, \\ \rho(0, x) = \begin{cases} \rho_j & \text{if } x < x_j, \\ \rho_{j+1} & \text{if } x > x_j, \end{cases} \\ j \neq 0, \end{cases} \quad (13)$$

where y_n satisfies

$$\begin{cases} \dot{y}_n(t) = \omega(\rho^n(t, y_n(t)+)), \\ y_n(0) = y_o. \end{cases} \quad (14)$$

Note that the solutions to the constrained Riemann problem in (13), left, coupled with (14), is constructed by means of \mathcal{R}^α , see Definition 3.1.

The approximate solution ρ^n constructed above can be prolonged up to the first time $\bar{t} > 0$, where two discontinuities collide, or a discontinuity hits the bus trajectory. In both cases, a new Riemann problem arises and its solution, obtained in the former case with \mathcal{R} and in the latter case with \mathcal{R}^α , allows to extend ρ^n further in time.

4.2. Bounds on the total variation

Given an approximate solution $\rho^n = \rho^n(t, \cdot)$ constructed by the wave-front tracking method, we define the Glimm type functional

$$\Upsilon(t) = \Upsilon(\rho^n(t, \cdot)) = \text{TV}(\rho^n) + \gamma = \sum_j |\rho_{j+1}^n - \rho_j^n| + \gamma, \quad (15)$$

where γ is given by

$$\gamma = \gamma(t) = \begin{cases} 0 & \text{if } \rho^n(t, y_n(t)-) = \hat{\rho}_\alpha, \rho^n(t, y_n(t)+) = \check{\rho}_\alpha \\ 2|\hat{\rho}_\alpha - \check{\rho}_\alpha| & \text{otherwise.} \end{cases} \quad (16)$$

The value of γ is chosen to get the following interaction estimates.

Lemma 2. *For any $n \in \mathbb{N}$, the map $t \mapsto \Upsilon(t) = \Upsilon(\rho^n(t, \cdot))$ at any interaction either decreases by at least 2^{-n} , or remains constant and the number of waves does not increases.*

Lemma 2 in particular implies that the wave-front tracking procedure can be prolonged to any time $T > 0$.

PROOF. In order to obtain a uniform bound on the total variation we will consider the different types of interactions separately. In particular, it is not restrictive to assume that at any interaction time $t = \bar{t}$ either two waves interact or a single wave hits the bus trajectory.

- (I1) We consider a classical collision between two waves (see Figure 5). In this case either two shocks collide (which means that the number of waves diminishes) or a shock and a rarefaction cancel. In any case, $\text{TV}(\rho^n)$ is not increasing and γ is constant and we get $\Upsilon(\bar{t}+) \leq \Upsilon(\bar{t}-)$.

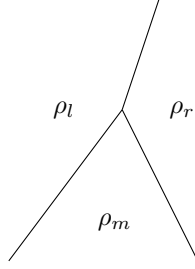


Figure 5: Interaction between two waves away from the bus trajectory.

A particular case is when the bus trajectory coincides with one of the interacting waves. In this case the wave must be a classical shock between a left state belonging to $[0, \check{\rho}_\alpha]$ and a right state in $[\hat{\rho}_\alpha, \rho^*]$, and it must move with speed equal to V_b . This interaction cannot generate a non-classical shock, therefore it can be treated as the general case above.

- (I2) Assume that a wave between two states $\rho_l, \rho_r \in [0, \check{\rho}_\alpha] \cup [\hat{\rho}_\alpha, 1]$ hits the bus trajectory (see Figure 6). In this case the front crosses the bus trajectory and no new wave is created. Notice that this collision may eventually lead to a modification of the bus trajectory (for example, if $\rho_r > \rho^*$, after the collision the bus takes the velocity $v(\rho_r) \neq \omega(\rho_l)$). In any case, $\text{TV}(\rho^n)$, Υ and the number of waves remain constant.

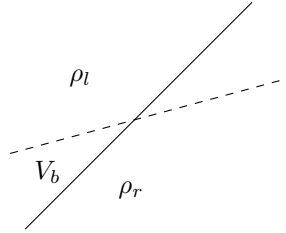


Figure 6: Interaction between a wave and the bus trajectory.

- (I3) Assume that we are in the presence of the non-classical shock along the bus trajectory. Different types of interactions may occur.
- (I3.1) Assume the non-classical shock is present at $t < \bar{t}$, and a shock between $\rho_l \in [0, \check{\rho}_\alpha]$ and $\hat{\rho}_\alpha$ hits the bus trajectory on the left (Figure 7a). After the collision, the number of discontinuities in ρ^n diminishes and the functional Υ remains constant:

$$\begin{aligned} \Delta \Upsilon(\bar{t}) &= \Upsilon(\bar{t}+) - \Upsilon(\bar{t}-) \\ &= |\rho_l - \check{\rho}_\alpha| + 2|\hat{\rho}_\alpha - \check{\rho}_\alpha| - (|\rho_l - \hat{\rho}_\alpha| + |\hat{\rho}_\alpha - \check{\rho}_\alpha|) \\ &= 0. \end{aligned}$$

Assume now a shock between $\check{\rho}_\alpha$ and $\rho_r \in [\hat{\rho}_\alpha, 1]$ hits the bus trajectory on the right (Figure 7b). Then, after the collision, the bus assumes the velocity $v(\rho_r)$ of the traffic mainstream, the number of discontinuities in ρ^n diminishes and the functional Υ remains constant:

$$\begin{aligned}\Delta\Upsilon(\bar{t}) &= \Upsilon(\bar{t}+) - \Upsilon(\bar{t}-) \\ &= |\hat{\rho}_\alpha - \rho_r| + 2|\hat{\rho}_\alpha - \check{\rho}_\alpha| - (|\check{\rho}_\alpha - \rho_r| + |\hat{\rho}_\alpha - \check{\rho}_\alpha|) \\ &= 0.\end{aligned}$$

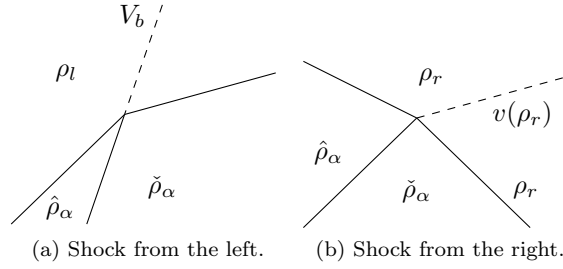


Figure 7: Interaction between a shock and the bus trajectory.

(I3.2) Consider now the case of a non-classical shock arising at $t = \bar{t}$. We first analyze the case of a rarefaction front hitting the bus trajectory from the left (Figure 8a). We have $\rho_r = \check{\rho}_\alpha < \rho_l \leq \hat{\rho}_\alpha$. In this case

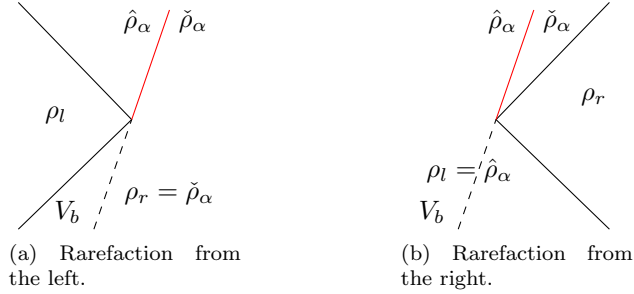


Figure 8: Interaction between a rarefaction and the bus trajectory.

new waves are created at \bar{t} and the total variation is given by:

- $\text{TV}(\bar{t}-) = |\check{\rho}_\alpha - \rho_l| \geq 2^{-n-1}$;
- $\text{TV}(\bar{t}+) = |\hat{\rho}_\alpha - \check{\rho}_\alpha| + |\hat{\rho}_\alpha - \rho_l| \leq 2|\hat{\rho}_\alpha - \check{\rho}_\alpha|$,

where the second estimate is obtained by simple algebraic manipulation of the total variation $\text{TV}(\bar{t}+)$. Then we are able to compute the

changes in the functional as follows:

$$\begin{aligned}\Delta\Upsilon(\bar{t}) &= \Upsilon(\bar{t}+) - \Upsilon(\bar{t}-) \\ &= (|\hat{\rho}_\alpha - \check{\rho}_\alpha| + |\hat{\rho}_\alpha - \rho_l|) - (|\check{\rho}_\alpha - \rho_l| + 2|\hat{\rho}_\alpha - \check{\rho}_\alpha|) \\ &= 2(\check{\rho}_\alpha - \rho_l) \leq -2^{-n},\end{aligned}$$

hence the functional is strictly decreasing.

Let us consider now the case of a rarefaction front hitting the bus trajectory from the right (Figure 8, right). In this case we have $\check{\rho}_\alpha \leq \rho_r < \rho_l = \hat{\rho}_\alpha$. A new wave is created at \bar{t} and the total variation is given by:

- $\text{TV}(\bar{t}-) = |\hat{\rho}_\alpha - \rho_r| \geq 2^{-n-1}$;
- $\text{TV}(\bar{t}+) = |\hat{\rho}_\alpha - \check{\rho}_\alpha| + |\check{\rho}_\alpha - \rho_r| \leq 2|\hat{\rho}_\alpha - \check{\rho}_\alpha|$,

The functional changes as follows:

$$\begin{aligned}\Delta\Upsilon(\bar{t}) &= \Upsilon(\bar{t}+) - \Upsilon(\bar{t}-) \\ &= (|\hat{\rho}_\alpha - \check{\rho}_\alpha| + |\check{\rho}_\alpha - \rho_r|) - (|\hat{\rho}_\alpha - \rho_r| + 2|\hat{\rho}_\alpha - \check{\rho}_\alpha|) \\ &= 2(\hat{\rho}_\alpha - \rho_r) \leq -2^{-n},\end{aligned}$$

making the functional strictly decreasing.

4.3. Convergence of approximate solutions

In this section we prove that the limit of wave-front tracking approximations provides a solution (ρ, y) of the PDE-ODE model (5) in the sense of Definition 4.1.

We start showing the convergence of the wave-front tracking approximations.

Lemma 3. *Let ρ^n and y_n , $n \in \mathbb{N}$, be the wave-front tracking approximations to (5) constructed as detailed in Section 4.1, and assume $\text{TV}(\rho_o) \leq C$ be bounded, $0 \leq \rho_o \leq 1$. Then, up to a subsequence, we have the following convergences*

$$\rho^n \rightarrow \rho \quad \text{in } \mathbf{L}_{\text{loc}}^1(\mathbb{R}^+ \times \mathbb{R}; [0, 1]); \quad (17a)$$

$$y_n(\cdot) \rightarrow y(\cdot) \quad \text{in } \mathbf{L}^\infty([0, T]; \mathbb{R}), \text{ for all } T > 0; \quad (17b)$$

$$\dot{y}_n(\cdot) \rightarrow \dot{y}(\cdot) \quad \text{in } \mathbf{L}^1([0, T]; \mathbb{R}), \text{ for all } T > 0; \quad (17c)$$

for some $\rho \in \mathcal{C}^0(\mathbb{R}^+; \mathbf{L}^1 \cap BV(\mathbb{R}; [0, 1]))$ and $y \in \mathbf{W}^{1,1}(\mathbb{R}^+, \mathbb{R})$.

PROOF. Lemma 2 gives a uniform bound on the total variation of approximate solutions: $\text{TV}(\rho^n(t, \cdot)) \leq \Upsilon(t) \leq \Upsilon(0)$. A standard procedure based on Helly's Theorem (see [5, Theorem 2.4]) ensures the existence of a subsequence converging to some function $\rho \in \mathcal{C}^0(\mathbb{R}^+; \mathbf{L}^1 \cap BV(\mathbb{R}; [0, 1]))$, proving (17a).

Since $|\dot{y}_n(t)| \leq V_b$, the sequence $\{y_n\}$ is uniformly bounded and equicontinuous on any compact interval $[0, T]$. By Ascoli-Arzelà Theorem, there exists a subsequence converging uniformly, giving (17b).

In order to prove (17c), we have to show that $\text{TV}(\dot{y}_n; [0, T])$ is uniformly bounded. In fact, the analysis performed in Section 4.2 shows that \dot{y}_n can change only at interactions with waves coming from its right. We can estimate the speed variation at interactions times \bar{t} by the size of the interacting front:

$$|\dot{y}_n(\bar{t}+) - \dot{y}_n(\bar{t}-)| = |\omega(\rho_l) - \omega(\rho_r)| \leq |\rho_l - \rho_r|.$$

In particular, \dot{y}_n is non-increasing at interactions with shock fronts and non-decreasing at interactions with rarefaction fronts, which must be originated at $t = 0$. In fact, the analysis performed in Section 4.2 shows that no new rarefaction front can arise at interactions. Therefore,

$$\text{TV}(\dot{y}_n; [0, T]) \leq 2 \text{PV}(\dot{y}_n; [0, T]) + \|\dot{y}_n\|_{\mathbf{L}^\infty([0, T])} \leq 2 \text{TV}(\rho_o) + V_b$$

is uniformly bounded. Above, $\text{PV}(\dot{y}_n; [0, T])$ denotes the positive variation of \dot{y}_n , i.e. the total amount of positive jumps in the interval $[0, T]$.

4.3.1. Proof of (12a) and (12b)

Since ρ^n converge strongly to ρ in $\mathbf{L}_{\text{loc}}^1(\mathbb{R}^+ \times \mathbb{R}; [0, 1])$, it is straightforward to pass to the limit in the weak formulation of the conservation law, proving that the limit function ρ satisfies (12a). Kruzhkov entropy condition (12b) can be recovered in the same way.

4.3.2. Proof of (12c) and (12d)

We will prove that

$$\lim_{n \rightarrow \infty} \rho^n(t, y_n(t)+) = \rho^+(t) = \rho(t, y(t)+) \quad \text{for a.e. } t \in \mathbb{R}^+. \quad (18)$$

By pointwise convergence a.e. of ρ^n to ρ , there exists a sequence $z_n \geq y_n(t)$ such that $z_n \rightarrow y(t)$ and $\rho^n(t, z_n) \rightarrow \rho^+(t)$.

For a.e. $t > 0$, the point $(t, y(t))$ is for $\rho(t, \cdot)$ either a continuity point, or it belongs to a discontinuity curve (represented by $y(\cdot)$) that can be either a classical shock or a non-classical discontinuity between $\rho(t, y(t)-) = \hat{\rho}_\alpha$ and $\rho(t, y(t)+) = \check{\rho}_\alpha$.

Fix $\epsilon^* > 0$ and assume $\text{TV}(\rho(t, \cdot);]y(t) - \delta, y(t) + \delta]) \leq \epsilon^*$, for some $\delta > 0$. Then by weak convergence of measures (see [6, Lemma 15]) we have $\text{TV}(\rho^n(t, \cdot);]y(t) - \delta, y(t) + \delta]) \leq 2\epsilon^*$ for n large enough, and we can estimate

$$|\rho^n(t, y_n(t)+) - \rho^+(t)| \leq |\rho^n(t, y_n(t)+) - \rho^n(t, z_n)| + |\rho^n(t, z_n) - \rho^+(t)| \leq 3\epsilon^*$$

for n large enough.

If $\rho(t, \cdot)$ has a discontinuity of strength greater than ϵ^* at $y(t)$, then also $|\rho^n(t, y_n(t)+) - \rho^n(t, y_n(t)-)| \geq \epsilon^*/2$ for n sufficiently large, and we proceed as in [6, Section 4]. That is, we set $\rho^{n,+} = \rho^n(t, y_n(t)+)$ and we show that for each $\varepsilon > 0$ there exists $\delta > 0$ such that for all n large enough there holds

$$|\rho^n(s, x) - \rho^{n,+}| < \varepsilon \quad \text{for } |s - t| \leq \delta, |x - y(t)| \leq \delta, x > y_n(s). \quad (19)$$

In fact, if (19) does not hold, we could find $\varepsilon > 0$ and sequences $t_n \rightarrow t$, $\delta_n \rightarrow 0$ such that $\text{TV}(\rho^n(t_n, \cdot); [y_n(t_n), y_n(t_n) + \delta_n]) \geq \varepsilon$. By strict concavity of the flux function f , there should be a uniformly positive amount of interactions in an arbitrarily small neighborhood of $(t, y(t))$, giving a contradiction. Therefore (19) holds and we get

$$|\rho^n(t, y_n(t)+) - \rho^+(t)| \leq |\rho^n(t, y_n(t)+) - \rho^n(t, z_n)| + |\rho^n(t, z_n) - \rho^+(t)| \leq 2\varepsilon$$

for n large enough, thus proving (18). Combining (17c) and (18) we get $\dot{y}(t) = \omega(\rho(t, y(t)+))$ for a.e. $t > 0$.

In order to verify that the limit solutions satisfy the constraint (12d), we can use directly (18) and the fact that wave-front tracking approximations satisfy the constraint (4) by construction.

Acknowledgments

This research was supported by the European Research Council under the European Union's Seventh Framework Program (FP/2007-2013) / ERC Grant Agreement n. 257661.

References

- [1] Andreianov, B., Goatin, P., Seguin, N., 2010. Finite volume schemes for locally constrained conservation laws. Numer. Math. 115 (4), 609–645, with supplementary material available online.
URL <http://dx.doi.org/10.1007/s00211-009-0286-7>
- [2] Borsche, R., Colombo, R., Garavello, M., 2012. Mixed systems: Odes - balance laws. Journal of Differential equations 252, 2311–2338.
- [3] Borsche, R., Colombo, R. M., Garavello, M., 2010. On the coupling of systems of hyperbolic conservation laws with ordinary differential equations. Nonlinearity 23 (11), 2749–2770.
URL <http://dx.doi.org/10.1088/0951-7715/23/11/002>
- [4] Bressan, A., 1988. Unique solutions for a class of discontinuous differential equations. Proc. Amer. Math. Soc. 104 (3), 772–778.
URL <http://dx.doi.org/10.2307/2046790>
- [5] Bressan, A., 2000. Hyperbolic systems of conservation laws. Vol. 20 of Oxford Lecture Series in Mathematics and its Applications. Oxford University Press, Oxford, the one-dimensional Cauchy problem.
- [6] Bressan, A., LeFloch, P. G., 1999. Structural stability and regularity of entropy solutions to hyperbolic systems of conservation laws. Indiana Univ. Math. J. 48 (1), 43–84.
URL <http://dx.doi.org/10.1512/iumj.1999.48.1524>

- [7] Bressan, A., Shen, W., 1998. Uniqueness for discontinuous ODE and conservation laws. *Nonlinear Anal.* 34 (5), 637–652.
URL [http://dx.doi.org/10.1016/S0362-546X\(97\)00590-7](http://dx.doi.org/10.1016/S0362-546X(97)00590-7)
- [8] Chalons, C., Goatin, P., Seguin, N., 2013. General constrained conservation laws. application to pedestrian flow modeling. *Netw. Heterog. Media* 8 (2), 433–463.
- [9] Colombo, R. M., Goatin, P., 2007. A well posed conservation law with a variable unilateral constraint. *J. Differential Equations* 234 (2), 654–675.
- [10] Colombo, R. M., Marson, A., 2003. A Hölder continuous ODE related to traffic flow. *Proc. Roy. Soc. Edinburgh Sect. A* 133 (4), 759–772.
URL <http://dx.doi.org/10.1017/S0308210500002663>
- [11] Daganzo, C., Laval, J. A., 2004. Moving bottlenecks: A numerical method that converges in flows. *Transportation Research Part B* 39, 855–863.
- [12] Daganzo, C., Laval, J. A., 2005. On the numerical treatment of moving bottlenecks. *Transportation Research Part B* 39, 31–46.
- [13] Delle Monache, M. L., Goatin, P., 2014. A front tracking method for a strongly coupled pde-ode system with moving density constraints in traffic flow. *Discrete Contin. Dyn. Syst. Ser. S* 7 (3), 435–447.
- [14] Filippov, V. V., 1994. Ordinary differential equations with discontinuous right-hand sides. Vol. 30. Kluwer academic Publisher.
- [15] Garavello, M., Goatin, P., 2011. The Aw-Rascle traffic model with locally constrained flow. *J. Math. Anal. Appl.* 378 (2), 634–648.
URL <http://dx.doi.org/10.1016/j.jmaa.2011.01.033>
- [16] Giorgi, F., 2002. Prise en compte des transports en commun de surface dans la modélisation macroscopique de l’écoulement du trafic. Ph.D. thesis, Institut National des Sciences Appliquées de Lyon.
- [17] Kruzhkov, S. N., 1970. First order quasilinear equations with several independent variables. *Mat. Sb. (N.S.)* 81 (123), 228–255.
- [18] Lattanzio, C., Maurizi, A., Piccoli, B., 2011. Moving bottlenecks in car traffic flow: a PDE-ODE coupled model. *SIAM J. Math. Anal.* 43 (1), 50–67.
URL <http://dx.doi.org/10.1137/090767224>